Demonstration of LiDAR on Accurate Surface Damage Measurement: A Case of Transportation Infrastructure

Nikunj Dhanani[1], Vignesh V P[2], Senthilkumar Venkatachalam[3]
[1,2,3]Department of Civil Engineering, Indian Institute of Technology, Palakkad - 678623, India
[1]102013002@smail.iitpkd.ac.in,[2]102214002@smail.iitpkd.ac.in, [3]senthil@iitpkd.ac.in

Abstract

Accurate damage measurements of the transport infrastructure facilities during their maintenance/service life are characterized by their higher cost, safety hazards, historical data loss etc. Conventional techniques such as active sensing equipment and manual visual inspection have limitations on their longevity and sustainability. To overcome this, many non-contact measurement technologies such as photogrammetric techniques, LiDAR etc., are demonstrated in various measurement-related applications. However, measurement accuracy in these photogrammetric techniques is affected by many external factors, which discourage their wider usage as preferable measurement techniques. Many of these factors cannot be controlled by the surveyor/operator on the ground, but the scanner location plays a significant role in the accuracy of the collected point cloud data. Also, there exist minimal guidelines on the scanner placement with respect to the accuracy of measurements. Hence, there is a need for a guiding method to appropriately place the LiDAR towards achieving the targeted accuracy level. With this background, the study developed mathematical equations to understand the variation of point cloud density with respect to the location of LiDAR from the target surface. An interaction diagram is developed to accurately predict the effective scan area, with anticipated point cloud density/point spacing. A non-contact LiDAR-based measurement framework has been developed as part of this research. However, this paper only has the scope to elaborate on the evaluation of the developed framework's accuracy through a case study on an old bridge structure with surface damage. The study was carried out on a straight and curved surface of the piers by placing the LiDAR at appropriate guiding locations from the target surfaces, with varying orientations to the scan surface. Upon post-processing the collected point cloud data, it is concluded that the proposed scan area planning framework using LiDAR can detect surface damages as little as 3mm on the highway bridge components accurately.

Keywords – LiDAR; Scan area planning; Surface damage assessment.

1 Introduction

Damages due to environmental and human factors are inevitable to any structural component that causes distress to the whole structural system. According to a report by Indian Bridge Management System (IBMS), more than 137 bridges were classified as distressed, which emphasizes the importance of timely maintenance and early damage detection intervention to extend the life and serviceability of the structural system [1,2]. Traditionally, periodic monitoring of the bridge is done by employing conventional diagnostic methods which include the active strain gauge or through the inspector's visit. Relatively, all the above-mentioned distressed bridge structures are constructed a long time ago, the effectiveness of the active devices on the bridge members is not capturing the damages and hence the inspectors visit the site periodically and perform visual inspections. Based on the inspector's subjective assessment of damages, various Non-Destructive Tests (NDT) such as the ultrasonic pulse velocity test, rebound hammer test, penetration method, and many other tests are performed [3]. Despite high accuracy, these methods require the deployment of costly special types of equipment, such as an 'under-bridge inspection truck' to access the damages. Due to this reason, the assessment is performed only on the critically damaged areas instead in an exhaustive, periodic, and proactive manner. In addition, it is a challenge to inspect and measure the progressive damages in the same area over a period of time, as there are no accurate historical data to compare with, but the subjective assessment statements by the experts. Therefore, employing a digitalised non-contact proactive monitoring method may overcome the limitations associated with these traditional inspection-based assessments and monitoring [4,5].

Evidently, Digital imaging and Three-dimensional (3D) laser scanning or otherwise LiDAR is considered as most effective non-contact measurement technologies for rapid and precise detection of preliminary structure damages [6]. In both Photogrammetry and LiDAR, the structure is captured as a 3D point cloud data, which is

generally defined in a cartesian coordinate system (X, Y, and Z) along with RGB colour values. Image-based acquisition of 3D point clouds using robotic equipment such as UAVs/drones has created vast new prospects for rapid and detailed 3D point cloud generation. These point cloud data are then utilized for structural damage detection through Multiview-Stereo (MVS), Structure-from-Motion (SfM) and other photogrammetry-based algorithms [7,8,9]. However, in the case of photogrammetry, for large-scale structures such as bridges, the image quality is influenced by many factors such as the surrounding environmental conditions, distortion, etc., and it is time-consuming [10]. But the deployment of 3D laser scanning technology shows advantages in terms of processing time and data quality [11]. LiDAR technology is demonstrated to monitor large-scale non-moving structures such as bridges, tunnels, etc., on a temporal basis [12], however, its wider application has not been realized due to many reasons. It collects data over time to detect structural changes due to events like seasonal variations, accidental impact, and natural calamities such as earthquakes, landslides, heavy rain, etc. The laser scanner units are primarily classified based on their data-capturing modes, such as aerial, mobile, and terrestrial. Although each of these LiDAR data collection methods has its own advantages and limitations, the terrestrial is more common and widely adopted in collecting data on structures and their components such as cracks and deformations over a period of time [13].

As seen in Figure 1, Terrestrial Laser Scanner (TLS) scans the surface by locating millions of points in vertical parallel lines. It rotates by an angle $\Delta\emptyset$ along a horizontal plane to cover the vendor-specified scan area along the plane and, then it rotates along the vertical plane by an incremental angle of $\Delta\theta$ to cover the specified coverage range. The distance covered by rotating the angles $\Delta\emptyset$ and $\Delta\theta$ is known as interpoint spacing which is denoted by a_h and a_v as shown in Figure 1. In order to detect structural damages on a millimetre scale, it is necessary to obtain interpoint spacing of the point cloud in a similar range. The interpoint spacing variations depend on many factors such as point cloud density, target surface distance from the scanner location, scan resolution, atmospheric conditions, object surface properties, scanning geometry, instrument mechanism etc., [14]. Among these factors, the scanner position and orientation are the only factors that can be controlled by the operator in the field.

Further, the scanning geometry is significantly influenced by the distance and orientation of the scanned surface concerning the scanner position, 'D' in Figure 1(A). Therefore, the location of the scanner plays a significant role in the point cloud density. Therefore, the main aim of this study is to obtain a sufficiently denser point cloud, to detect surface damages of desired accuracy with an appropriate scanner location from the scan target surface. The proposed-scan area planning task in this study is divided into two steps. The first step is the determination of the Field of View (FOV) calculation from a particular TLS location. Second, the calculation of interpoint spacing variation within the estimated FOV. In this regard, Anil et al. [15] conducted several lab experiments to identify the limits of laser scanners for damage assessment of reinforced concrete buildings. Also, Anil et al. demonstrated their study using vendor-provided post-processing tools and guidelines. In a related context, Chen et al. [16] and Fras et al. [17] developed a 2-D model-based scan planning approach to estimate the horizontal FOV of an existing building using vendor-provided post-processing tools. Furthermore, Biswasa et al. [18] and Wakisaka et al. [19] developed a 3-D model-based scan planning approach to estimate the horizontal as well as vertical FOV of a structure.

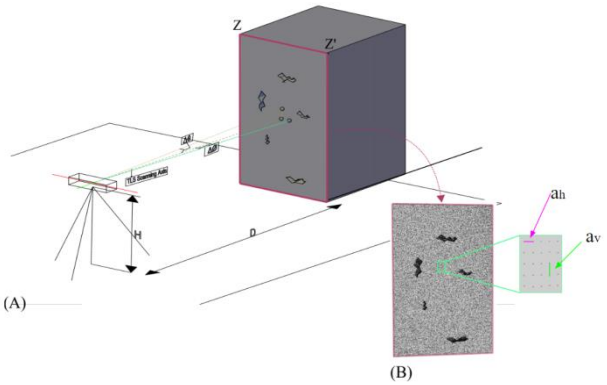

Figure 1: (A) Scanning of pier front side ZZ' using TLS. (B) Scanned point cloud of side ZZ'

From the literature, it is evident that most of the previous studies were primarily focused on FOV determination without much emphasis on the accuracy of the collected data. However, to accurately capture minor damages on the surface of the structural components, it is necessary to have the appropriate interpoint spacing in the collected point cloud data. In addition to this, most of these past studies have validated the developed FOV approach in a lab environment. Thus, in this paper authors attempted to validate the developed framework through a field experiment to ascertain the accuracy of the proposed framework. The research adopted three steps procedures viz. 1) Development of the scanning FOV framework through mathematical equations and guiding interaction diagrams to the field operators. 2) An experiment in a controlled/lab environment. 3) A field experiment to validate the developed framework. Since the first two steps of this research were published in a

previous article [20] and due to the limitations on the length of the manuscript, the explanation of the same is not included within the scope of this paper. The readers are strongly recommended to refer to the article in case more explanation is needed to understand the first two steps adopted in this research. The paper is organized as follows. The following section discusses the brief about the first two steps of the developed scan area planning framework for surface damage assessment. Section 3 outlines the methodology adopted for conducting the field experiment. Further sections describe the details of the case study and the experiment. The manuscript ends with the inferences from the obtained results, discussions, and conclusions.

2 Development of framework and Validation in a Controlled Environment

The interpoint spacings (a_h, a_v) increment depends upon the length of the scan plane from the scanning axis (i.e. L_X, L_Z), scanner's horizontal and vertical angular increment capability (i.e., $\Delta\theta$, $\Delta\emptyset$), and its distance from the surface (D) as depicted in Figure 2.

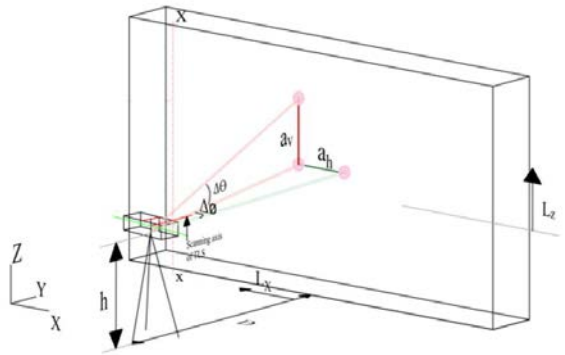

Figure 2. Scanning the surface perpendicular to the scanning axis of the TLS

The following equations are derived for a straight scanning surface perpendicular to the scanning axis using a simple trigonometrical relationship,

$$L_{X'} = [(\tan(\tan^{-1}(L_X/D) + \Delta\emptyset)) \times D] \quad \ldots\ldots\ldots\ldots\ldots\ldots (1)$$

$$a_h = (L_{X'} - L_X) \quad \ldots\ldots\ldots\ldots\ldots\ldots\ldots\ldots\ldots\ldots\ldots\ldots (2)$$

$$R = \sqrt{((L_{X'})^2 + D^2)} \quad \ldots\ldots\ldots\ldots\ldots\ldots\ldots\ldots\ldots\ldots\ldots\ldots (3)$$

$$a_v = [(\tan(\tan^{-1}(L_Z/R) + \Delta\theta)) \times R] - L_Z \quad \ldots\ldots\ldots\ldots\ldots\ldots (4)$$

Similarly, a total of 19 mathematical equations are formulated for scanning the straight and curved surfaces by locating TLS parallel and perpendicular to them. Also, the interaction diagrams as shown in Figures 3 and 4 for all the above-mentioned combinations are also generated to guide the surveyor/operator in fixing the FOV and for identifying the appropriate scanner location to obtain the required interpoint spacing.

From the graphs in Figures 3 and 4, it has been inferred that the TLS can be located anywhere between 3m to 10m from the target surface to cover a scanning area of 5.4m × 4.9m ($L_X \times L_Z$) with a interpoint spacing as little as 2mm.

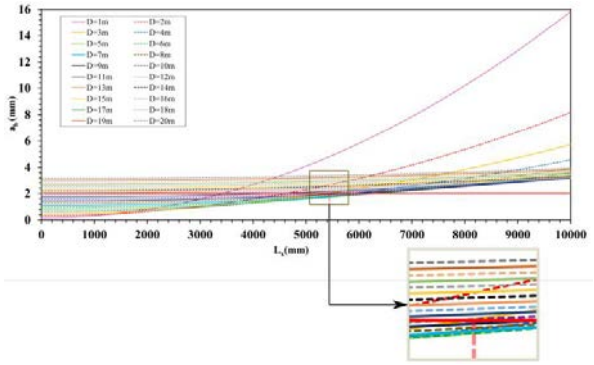

Figure 3. Variation of interpoint spacing a_h along the horizontal length (L_X) with different TLS distance (D) at 0.009◦ TLS incremental angle ($\Delta\emptyset$)

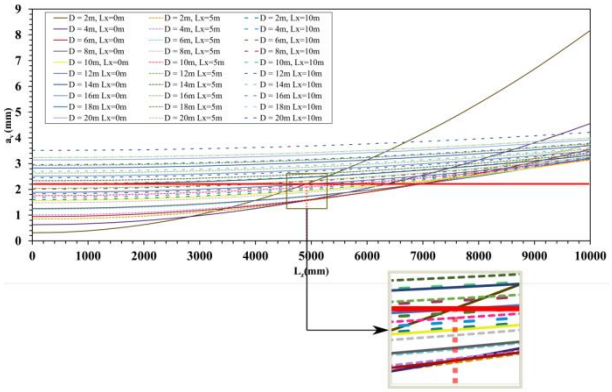

Figure 4. Variation of inter-point spacing a_v along the vertical length (L_Z) with different TLS distance (D) at 0.009° TLS incremental angle ($\Delta\theta$)

For validating the developed Scan Area Planning framework, experiments were conducted in a controlled/lab environment. Using interactive graphs, it was found that for a scan perpendicular to the target surface, to cover an area of about 5.4m x 4.9m (L_X x L_Z), the TLS shall be placed anywhere between 3m to 10m from the scanning surface. Average interpoint spacing differs by approximately 0.04mm from the measured value from the experiment and the predicted value based on the formula developed. Similarly, for other cases also, with the help of interactive graphs, the scan area and location of TLS can be predicted for aimed accuracy. The obtained results' accuracy motivated the authors to experiment with the same in a real-world setup, with all the other external factors.

3 Field Experiment Methodology

After the controlled environment experiments, the field experiment location was identified. The authors visited many bridge sites in and around the institute and with the help of a local public works organization identified the Velanthavalam bridge site shown in Figure 5.

This bridge was constructed in 1986 over a river (Kumittipathi). It was located on the border connecting two states (Kerala and Tamil Nadu) in India. The bridge has round-nosed rectangle piers. Therefore, it is possible to demonstrate the framework's accuracy on both vertical straight and curved surfaces of planned scan area exercises. In addition, the bridge is accessible from most of the sides and has identifiable surface damages of varying sizes (many cracks of varying sizes on the straight and curved surfaces). Hence this site was selected to validate the crack detection accuracy for various distances of scanner locations from the surface.

Figure 5. Velanthavalam bridge site

For this field experiment, TLS specifications with horizontal and vertical angle increment of 0.009° and specifications of, range 0.6m to 350m, Field of view (horizontal/vertical): 360° / 300°, Min angular increment (horizontal/vertical): 0.009° / 0.009°, Laser wavelength: 1550nm and Measurement speed (pts/sec): 976,000 was used. The same scanner was also used for the controlled experiments. The field experiment has the below objectives.

1. To predict the distance and orientation of the scanner from the damaged surface using the proposed framework, which includes the TLS location calculated using the developed mathematical equation and interactive graphs.
2. To validate the interpoint spacing and measurement accuracy using the collected point cloud data of the vertical straight and curved surfaces of the damaged bridge pier.

The unit of analysis for this validation exercise is the crack width, length, etc., obtained from the point cloud data. The data collection includes scanning the vertical straight and curved surfaces while locating the scanner perpendicular to the damaged surface.

Based on the interaction diagram developed from the developed mathematical equations, it is suggested to place the scanner between 2 to 8 m distances to obtain an accuracy of more than 3 mm. The horizontal and vertical angle increment is assumed to be set as 0.009° during the experiment.

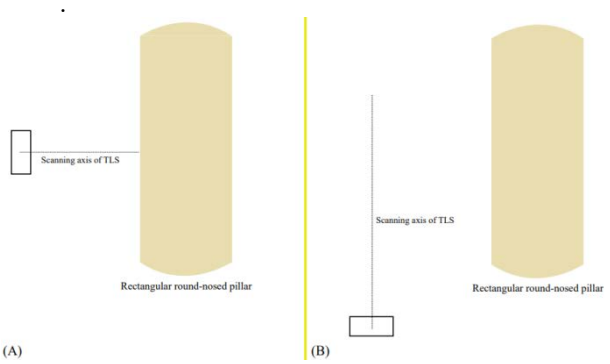

Figure 6. (A) TLS positioned perpendicular to the surface. (B) TLS positioned parallel to the surface

4 Validation of the scan area planning on Vertical Straight surfaces

Depending on accessibility, there were two possible locations for TLS placement towards scanning the pier's vertical straight surfaces. If the scanning surface is accessible, the scanner can be placed perpendicular to it (Figure 6 (A)). If not, it needs to be placed parallel to the surface (Figure 6 (B)).

As shown in Figure 7, the scanning is performed by placing the TLS at a 5m distance from the damaged surface. To validate the variation of the interpoint spacing, the value of a_h and a_v are measured at various points in the damaged surface (i.e., mentioned as A, B, C etc. in Fig. 7) along the horizontal and vertical axis (L_X and L_Z).

The interpoint spacing values calculated from the mathematical equations (C_V) and the measured interpoint spacing values (M_V) from the post-processing software are tabulated in Table 1. The difference between them is noticed in the range of 0.1 to 0.2 mm.

To validate the accuracy on measuring various damages, a comparison analysis is carried out in which each damage is measured using a vernier scale as shown in Fig. 8 and scanned point cloud data of the crack width and length. Table 2 compares the crack width value measured using the Vernier scale and the crack width value measured using scanned point cloud data.

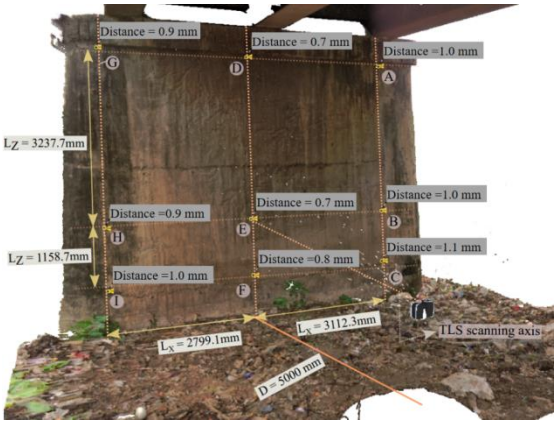

Figure 7 Measurement of point cloud spacing a_h, a_v along L_X & L_Z

Figure 8. (A) Scanned cracks using TLS (B) Measurement of crack 1 using Vernier scale

Similarly, the verification exercise is carried out for the scanner placed along the parallel plane of the scan axis. The same steps which are explained in the previous experiment, scanner placement on perpendicular to the scan surface are followed. Firstly, the value of a_h and a_v is measured at different sections along the length L_Y and L_Z (see Figure 9). Subsequently, a comparison table is prepared (see Table 1). Here also, the maximum difference between calculated (C_V) and measured values (M_V) of interpoint spacing was noticed in the range of 0.1mm to 0.2mm. Similarly, the crack width was measured using the post-processing tool and the Vernier scale (see Table 2), and the accuracy attained was around 2 mm which is better than, the targeted accuracy set before the field experiment (i.e., 3 to 5mm).

Figure 9 Measurement of point cloud spacing a_h, a_v along L_Y & L_Z

Table 1 Comparison of Interpoint Spacing in Field Environment

	Interpoint Spacing Value on a Plane Perpendicular to the Scanning Axis of TLS						Interpoint Spacing Value on a Plane Parallel to the Scanning Axis of TLS					
	a_h along lengths L_x and L_z			a_v along lengths L_x and L_z			a_h along lengths L_y and L_z			a_v along lengths L_y and L_z		
S_N	M_V	C_V	D_F	M_V	C_V	D_F	M_V	C_V	D_F	M_V	C_V	D_F
A	1	1.1047	0.1047	1.2	1.2192	0.0192	0.9	0.7854	0.1146	1.2	1.1131	0.0869
B	1	1.1047	0.1047	0.9	0.9456	0.0456	0.9	0.7854	0.1146	0.8	0.7568	0.0432
C	1.1	1.1047	0.0047	0.9	0.9807	0.0807	1	0.7854	0.2146	0.8	0.7435	0.0565
D	0.7	0.8091	0.1091	1.2	1.129	0.071	1.6	1.5141	0.0859	1.3	1.271	0.029
E	0.7	0.8091	0.1091	0.8	0.8094	0.0094	1.5	1.5141	0.0141	1.2	1.0145	0.1855
F	0.8	0.8091	0.0091	0.9	0.8504	0.0496	1.6	1.5141	0.0859	1.1	1.0048	0.0952
G	0.9	1.1048	0.2048	1.3	1.2019	0.0981	3.1	3.0996	0.0004	1.7	1.6019	0.0981
H	0.9	1.1048	0.2048	0.9	0.9211	0.0211	3.1	3.0996	0.0004	1.6	1.4227	0.1773
I	1	1.1048	0.1048	0.9	0.9571	0.0571	3.2	3.0996	0.1004	1.6	1.4161	0.1839

Note: S_N, M_V, C_V, D_F - Name of intersection points, Measured value, Calculated value, and their Difference respectively. All the values are in mm

Table 2 Accuracy comparison of crack width

	TLS perpendicular to the surface		TLS parallel to the surface	
S_N	W_{PCD}	W_{VS}	W_{PCD}	W_{VS}
Crack 1	23.3	24	22.3	24
Crack 2	55.6	55	55.2	55
Crack 3	36.7	35	35.2	35

Note: S_N, W_{PCD}, and W_{VS} – The name of cracks, measured of crack width using scanned point cloud and using Vernier scale respectively. All values are in mm

5 Validation of the scan area planning on Curved surfaces

From the earlier study [20] it was found that TLS can cover at least 90° of Pier 1's FOV (Visible quarter) and 45° of Pier 2's FOV as shown in Fig. 10 and 11. A similar FOV behavior is observed when scanning the curved portions of the piers at a distance of 3m perpendicular to the surface (see Figure 10).

As shown in Figure 11, the circular surface of the Pier is having varying diameters. Therefore, two sections (Section 1 at the bottom and Section 2 at the top) are selected to validate interpoint spacing variation behavior. At each section, the interpoint spacing value is checked at two locations (represented in blue and orange lines respectively in Fig.11). In Table 3, a comparison is made between the measured (M_V) and calculated values (C_V) at multiple locations and sections.

From the experiment, it was found that in Pier 1, some minor cracks were found, and its sizes range in mm. According to the developed model, if the scanner was placed 3m away, it would be able to detect cracks up to 1mm around the 0° location of the 1st pier. As seen in Figure 12, all minor cracks are captured accurately, and also the width captured by the TLS point cloud is compared with the Vernier scale measurement (Table 4). It is noticed that the difference between the calculated (W_{PCD}) and measured (W_{VS}) is in a fraction of a mm.

Figure 10: Scan coverage area while locating TLS perpendicular to the first pier

Table 3 Comparison of interpoint spacing ah at different sections of Pier 1 & 2

	S_N	N_L	M_V	C_V	D_F
Pier 1	**Section 1**	0° Location	0.4986	0.4953	0.0032
		90° Location	1.7111	1.8954	0.1843
	Section 2	0° Location	0.5511	0.4953	0.0557
		90° Location	2.4125	2.9681	0.5557
Pier 2	**Section 1**	0° Location	2.6032	2.5433	0.06
		90° Location	13.754	14.3866	0.6326
	Section 2	0° Location	2.677	2.5759	0.1011
		90° Location	13.574	13.6395	0.0655

Note: S_N, N_L, M_V, C_V and D_F -The sections name, location name, measured value, calculated value and Difference between two points respectively. All values are in mm

Figure 11. Measurement of point cloud interpoint spacing a_h, at each location of the pier section

Table 4 Accuracy comparison of crack width measured at Section 2 of Pier 1 (Fig. 11 and 12)

S_N	W_{PCD}	W_{VS}
Crack 1	2.7	3
Crack 2	2.9	3
Crack 3	34.6	33.3

Note:

S_N, W_{PCD}, and W_{VS} – the name of cracks, measured crack width using scanned point cloud and using Vernier scale respectively. All values are in mm

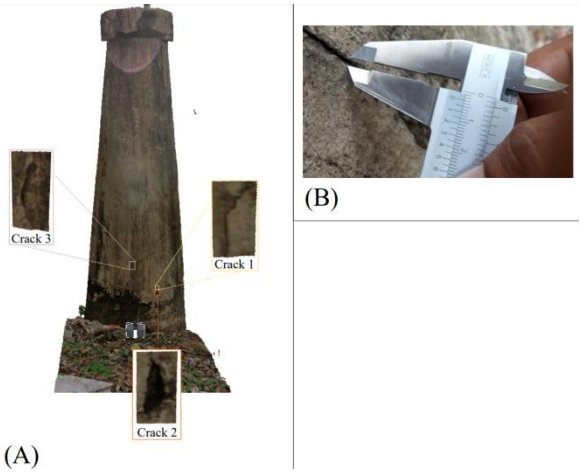

Figure 12 (A) Scanned cracks using TLS (B) Measurement of crack 1 using Vernier scale

6 Discussions

The point cloud interpoint spacing variations between the measured and calculated values in this experiment ranges between 0.0004mm to 1.7mm. The maximum variation occurs while locating TLS parallel to the surface at a 2m distance. It is advisable to keep the TLS as close and perpendicular as to the cracks. The height of the TLS can be limited between 1.2m to 1.6m for better ergonometric operations. The field experiment conducted during this study, chose a conducive external environment such as light, accessibility, etc., however, collecting data during less visibility and adverse weather conditions may reduce the data and measurement accuracy. Further, the study was conducted when there was no water in the causeway, however, the water in the causeway may affect the data collection about the submerged surfaces. The existing deformities and irregular geometrics have not been considered in this study. However, the same becomes insignificant when the temporal variations on the surface damages are assessed. The study may also demand fixing standard station points to obtain the data temporally over a period of time regularly. Furthermore, this study did not consider any economic or time benefit analysis, future experiments may include the same in order to compare with the conventional methods over the LiDAR-based technologies for their benefits.

7 Summary and Conclusions

This study developed a Scan Area Planning framework to collect point cloud data with the desired level of accuracy in identifying surface damages. The study aims to accurately collect minor structural damages using LiDAR technology. This paper summarizes the significant role of scanner location in obtaining point cloud data with the desired level of accuracy. The developed mathematical equations and generated interaction diagrams can be utilized as a guiding ready reckoner for the field surveyors/operators to fix the scanner location and orientation for collecting the appropriately suitable and accurate point cloud data. This paper further demonstrated validation methodology for the developed framework (reported in the previous study [20]) and concluded that the location and orientation of the scanner to the target surface itself could be controlled to obtain accurate surface damage measurement using the LiDAR point cloud. The experiments were aimed to capture the surface damages ranging from 3mm to 5mm. Nevertheless, the validation results indicate that around 1mm cracks were also captured using the developed models. The study has some limitations as the accuracy hasn't been checked with varying scanner positions and longer-range distances from the target surface. The interaction diagram was developed only up to 20m distance from the target in this study. Further, working under extreme weather conditions and temporal variations are not captured to claim the applicability with a wider scope. However, the authors are of the opinion to obtain similar results and are willing to experiment with the same in the near future. Collecting and storing this accurately measured point cloud data during the life cycle of the structural members may lead to capturing the progressive damages that the structural members may undergo and warrant a timely retrofitting which may increase and improve the life span and serviceability of the infrastructure facility.

Acknowledgement

The authors would like to acknowledge KHRI and Kerala PWD for their support to access the bridge site and funding for this research work.

References

[1] N. De Belie and E. Gruyaert, HEALCON-Conference-Self-Healing Concrete for Prolonged Lifetime, Delft, Nederland, 2016, pp. 1–5.

[2] Joshi, S. and Raju, S.S., 2018. Indian Bridge Management System-Overview and Way Forward. Maintenance, Safety, Risk, Management and Life-Cycle Performance of Bridges, pp.205-205.

[3] E. Niederleithinger, S. Gardner, T. Kind, R. Kaiser, M. Grunwald, G. Yang, B. Redmer, A. Waske, F. Mielentz, U. Effner et al., arXiv preprint arXiv:2008.07251, 2020.

[4] J. Thomas, A. Kareem and K. W. Bowyer, IEEE Transactions on geoscience and remote sensing, 2013, 52, 3851–3861.

[5] M. Abdo, A review book. Open Science, 2014.

[6] Truong-Hong, L., Falter, H., Lennon, D. and Laefer, D.F., 2016, January. Framework for bridge inspection with laser scanning. In EASEC-14 Structural Engineering and Construction, Ho Chi Minh City, Vietnam, 6-8 January 2016.
[7] S. Ullman, Proceedings of the Royal Society of London. Series B. Biological Sciences, 1979, 203, 405–426.
[8] A. Alfonso-Torreño, Á. Gómez-Gutiérrez, S. Schnabel, J. F. L. Contador, J. J. de Sanjosé Blasco and M. S. Fernández, Science of the Total Environment, 2019, 678, 369–382.
[9] D. Giordan, Y. Hayakawa, F. Nex, F. Remondino and P. Tarolli, Natural hazards and earth system sciences, 2018, 18, 1079–1096.
[10] C. Axel and J. A. van Aardt, Journal of Applied Remote Sensing, 2017, 11, 046024.
[11] D. Skarlatos and S. Kiparissi, 2012.
[12] S.-E. Chen, Laser Scanner Technology, 2012, 71.
[13] B. Riveiro, M. DeJong and B. Conde, Automation in Construction, 2016, 72, 258–268.
[14] S. Soudarissanane, R. Lindenbergh, M. Menenti and P. Teunissen, Proceedings ISPRS Workshop Laserscanning 2009,1-2 Sept 2009, Paris, France, Paris, France, 2009, pp. Vol. XXXVII, Part 3/W8.
[15] E. B. Anil, B. Akinci, J. H. Garrett and O. Kurc, ISARC. Proceedings of the International Symposium on Automation and Robotics in Construction, Montreal, Canada, 2013.
[16] M. Chen, E. Koc, Z. Shi and L. Soibelman, Automation in Construction, 2018, 93, 165–177.
[17] E. Frías, L. Díaz-Vilariño, J. Balado and H. Lorenzo, Remote Sensing, 2019, 11, 1963.
[18] H. K. Biswasa, F. Boschéa and M. Suna, Symposium on Automation and Robotics in Construction and Mining (ISARC 2015), Waterloo, Canada, 2015.
[19] E. Wakisaka, S. Kanai and H. Date, ISARC. Proceedings of the International Symposium on Automation and Robotics in Construction, Waterloo, Canada, 2019.
[20] N. Dhanani and S. Venkatachalam, CIB - Conference-Smart Built Environment, Dubai, United Arab Emirates, 2021, pp. 101–110